Terrestrial Propagation of 2-Gigahertz Emissions Transmitted from the Deep Space Network 70-Meter Antenna at Robledo

C. M. Ho,[1] M. K. Sue,[1] T. K. Peng,[2] and E. K. Smith[3]

This article presents a case study of potential interference from a 2-GHz transmitter in the Deep Space Network (DSN) station in Robledo, Spain, to the International Mobile Telecommunications (IMT)-2000 mobile receivers in the city of Madrid about 50 km away. This study has included the effect of terrain between Robledo and Madrid in evaluating the propagation modes, which include diffraction over the terrain, ducting through the atmosphere, and scattering by rain. It is a complete revision of a previous study wherein preliminary analysis of these phenomena was presented without taking the specific terrain into account. The predicted results concerning diffraction are consistent with measurements and with predictions of the Longley–Rice model. Because of attenuation by the hills, the expected power received through diffraction by a mobile receiver on ground level in Madrid is lower than the interference thresholds (−109 dBm) when the DSN antenna transmits at the normal power of 20 kW. The hills near the DSN antenna also provide much attenuation to the emissions propagated through atmospheric ducting. Considering the low duty cycle (12 percent or less) of about 2 GHz (S-band) transmissions at Robledo, the expected power of emissions propagated through atmospheric ducting does not exceed the receiver interference thresholds more than 0.1 percent of the time. The corresponding effect of rain scattering is estimated to be 0.01 percent of the time. These percentages decrease at larger distances.

I. Introduction

The International Mobile Telecommunications (IMT)-2000 [1–3], also known in Europe as the Universal Mobile Telecommunications System (UMTS) [6–8], and, in terms of technology, as the third-generation wireless [4], provides the 2110- to 2170-MHz band for use in the forward direction from the base station to mobile receivers [5,6]. The NASA Deep Space Network (DSN) has been operating high-power transmitters in the 2110- to 2120-MHz band according to the allocation of the International Telecommunication Union (ITU), with corresponding space-to-Earth receive frequencies in the 2290- to 2300-MHz band. These

[1] Communications Systems and Research Section.

[2] DSMS Plans and Commitments Program Office.

[3] University of Colorado, Boulder, Department of Electrical and Computer Engineering.

The research described in this publication was carried out by the Jet Propulsion Laboratory, California Institute of Technology, under a contract with the National Aeronautics and Space Administration.

transmitters are installed on the 34-m and 70-m antennas in the Deep Space Communications Complexes located at Goldstone in California, Canberra in Australia, and Robledo near Madrid, Spain. Because of the overlap of the two services in the 2110- to 2120-MHz band, it is necessary to understand the sharing conditions between the two services.

A preliminary analysis was conducted in late 1999 and early 2000 to outline the factors that must be considered in characterizing the potential interference from a DSN transmitter to the IMT-2000 mobile receivers in the neighborhood [12]. The analysis was intended to describe a general methodology of analysis for the first time in the DSN environment. It was not intended to provide a definitive estimation of interference. The study was conducted before measured results around Madrid were made available, and it did not take the local terrain into account. The present study is an update of the previous study. It has accounted for the terrain profile between Robledo and the city of Madrid, and its analytical results have been compared with measured data.

As described in the ITU propagation models [9–11], there are three significant modes of propagation in addition to radiation in the line of sight. They are diffraction over the spherical Earth and hilltops, ducting through atmospheric layers, and scattering by rain. While a transmitted wave can propagate through diffraction and ducting requires a low elevation angle (corresponding to the side lobe of a DSN antenna), they can also propagate by rain scattering with a large elevation angle.

This article presents an analysis using a detailed terrain profile between Robledo and Madrid and following the procedures described in ITU Recommendation ITU-R P.452 [9] and other ITU Recommendations [10,11]. Section II describes the path profile, including hilltops above the line of sight between the Robledo 70-m antenna and the city of Madrid. Section III estimates the power of signals propagating via terrain diffraction and received by the mobile receiver. The estimation is compared with actual measurements at Madrid and with predictions of the Longley–Rice model. Section IV estimates the power of signals propagated through atmospheric ducting, and Section V estimates the power of signals propagated through rain scattering. Section VI summarizes the results of Sections IV and V as a function of distance, and Section VII presents the conclusion.

II. Elevation Profile along the Path

A DSN 70-m antenna is located at Robledo, which is 44.7 km west of the city of Madrid (referenced to location R in Fig. 1, near the Royal Palace) and 47.3 km to the clock tower of Cibeles Palace (location M in Fig. 1, about 40 m above ground). The coordinates of the Robledo DSN transmitting antenna, reference point R in Madrid, and the clock tower of Cibeles Palace, location M, are given in Table 1. The 70-m antenna site is located within a valley, as shown in Fig. 2. We obtained the Robledo–Madrid elevation profile from the World Wide Terrain Database maintained by the Institute of Telecommunication Sciences (ITS). Because the profile had a limited spatial resolution of 1.0 km, some detailed features did not appear. Actually, there is a ridge consisting of two small peaks at 1.2 and 1.5 km east of the 70-m antenna, with an elevation angle of 1.5 deg for the first peak relative to the antenna. It therefore blocks the line of sight from the antenna to Madrid. With this modification, the elevation profile is given in Fig. 1. Reference location R in Madrid is in a valley, with a large highland in the west. The signals emitted from Robledo must propagate through diffraction over multiple obstacles before reaching Madrid.

III. Propagation by Diffraction

A. Modified Terrain Profile for Diffraction Analysis

1. Effective Earth Radius. Radio waves are bent when they propagate through atmospheric gases that decrease in density with altitude. The waves therefore can reach locations beyond the line of sight. The severity of the bending is determined by the gradient of the refractive index near the Earth's surface.

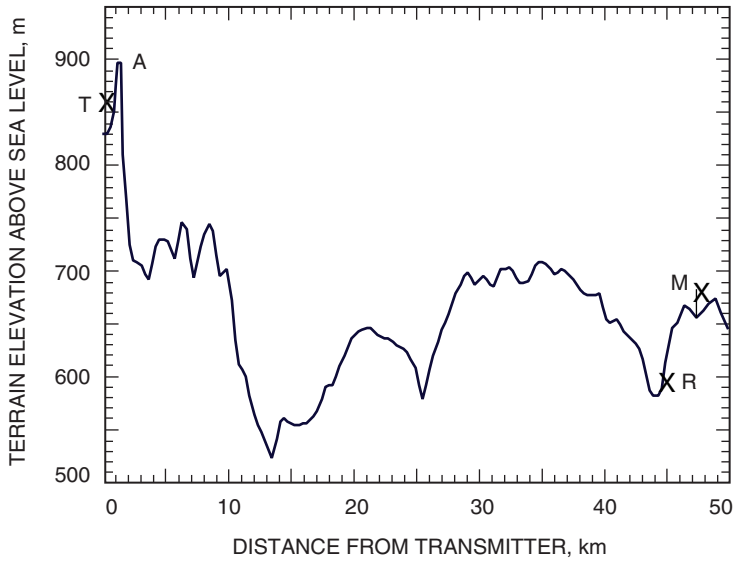

Fig. 1. Terrain profile from the Robledo antenna (location T) to Madrid: location R near the Royal Palace and location M at the top of the clock tower of Cibeles Palace. The profile is plotted on a flat Earth.

Table 1. Coordinates of three locations.

Location	Latitude	Longitude	Elevation, m
T, Robledo transmitter	40°254′52″ N	4°14′53″ W	865
R, near Royal Palace	40°25′1″ N	3°43′31″ W	587
M, tower of Cibeles Palace	40°25′06″ N	3°41′18″ W	680

Fig. 2. DSN antennas at Robledo and the surrounding hills: the 70-m antenna on the left and the ridges in the background at a higher elevation, blocking the view toward Madrid.

It is convenient for the sake of analysis to represent the radio ray as a straight line. For this reason, an "effective Earth radius" is defined that in effect stretches the Earth radius by a factor depending on the refractivity gradient, ΔN. The median (50 percentile) effective Earth radius factor k_{50} is defined as

$$k_{50} = \frac{157}{157 - \Delta N_{50}} \tag{1}$$

The median value of the effective Earth radius, a_e, is a product of the true Earth radius (6371 km at mid-latitude) and k_{50}:

$$a_e(50\%) = 6371 \times k_{50} \text{ (km)} \tag{2}$$

From the map of average annual ΔN values, $\Delta N_{50} = 45$ around the Madrid–Robledo area [9,10]. Thus, $k_{50} = 1.402$, and $a_e = 8931$ km.

2. Construction of the Path Elevation Profile. Using the effective Earth radius, we can modify the elevation of the terrain profile using the following equation:

$$y_i = h_i - \frac{x_i^2}{2a_e} \tag{3}$$

where y_i is the modified elevation, h_i is the terrain elevation above sea level, and x_i is the distance from the transmitter. The modified terrain profile is shown in Fig. 3, using the median effective Earth radius. All distances and heights are referenced to this modified plot.

To construct Fig. 3, elevations h_i of the terrain are read from topographic maps versus their distance, x_i, from the transmitting antenna. The terrain profiles, including terrain elevations and the sea level, have been adjusted according to the average curvature of the radio ray path. The solid curve near the bottom of the figure indicates the shape of the sea level of constant elevation ($h = 0$). The transmitter at location T and the receiver at location R have different horizons: hilltop A for the transmitter and point B for the receiver. The vertical scales of the figure are exaggerated in order to provide a sufficiently detailed representation of terrain irregularities.

B. Received Interference Power through Diffraction

We can estimate the interference power, P_r, received by a mobile receiver using the basic equation

$$P_r = P_t + G_t - L(p) + G_r \text{ (dB)} \tag{4}$$

Here, P_t is the transmitted power and G_t is the transmitter's antenna gain toward the physical horizon at an angle relative to the antenna boresight [15]. Diffraction losses, $L(p)$, from the transmitter at Robledo to receivers at location R and location M in Madrid are calculated in the Appendix using methods recommended by the ITU, and they include the effects of the terrain between Robledo and these locations. Here p is the percent of time when the DSN antenna is transmitting.

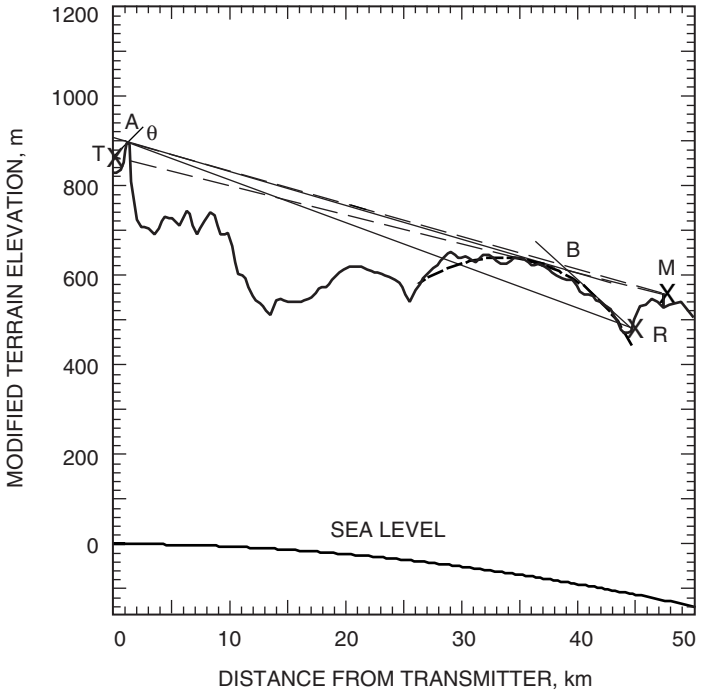

Fig. 3. Modified topographic terrain profile from Robledo to Madrid: location R in Madrid (Royal Palace) in the shadow of a large highland, and location M at the top of the clock tower of Cibeles Palace (east of location R) with a direct view of hilltop A. This profile has an effective radius a_e = 1.402 times the Earth radius.

1. Diffraction Losses. The statistical mean of diffraction loss, including the loss due to distance and the loss due to obstacles, is given below. Statistical variation due to atmospheric pressure gradients is small, within 3 dB:

$$L(50\%) = 234.4 \text{ dB from Robledo 70 m antenna to location R}$$

$$= 177.5 \text{ dB from Robledo 70 m antenna to location M}$$

2. IMT-2000 Mobile Receiver Characteristics. The IMT-2000 mobile station (MS) receiver has an antenna gain of 0 dBi. IMT-2000 systems are limited by interference (internal and external), with Gaussian noise playing a negligible role. An interference threshold for the Robledo emissions of 10 percent of the MS receiver total-noise-plus-interference floor of −98.9 dBm [24] has been considered, resulting in −108.9 dBm (10 dB below the receiver noise-plus-interference floor). This value represents a conservative value for the IMT-2000 downlinks (base station to mobiles).

3. DSN Transmitting Antenna Characteristics. The DSN 70-m antenna has a boresight gain of 62 dB and a back-lobe gain (>48 deg) of −10 dB [16]. The transmitter transmits 20 kW, or 73 dBm, during routine operation. It does not, however, transmit when the elevation angle is less than 10 deg, according to the ITU-R regulation. Hilltop A, the first obstacle to the east (only 1.2 km from the 70-m antenna), has a 1.5-deg elevation angle relative to the antenna dish center (whose first Fresnel distance, $D^2/2\lambda$, as seen in Fig. 4, is 17 km). When the transmitter is 10 deg above the horizon, its beam center has an 8.5-deg angle relative to the hilltop, corresponding to a gain of 5.7 dB. However, for the 70-m

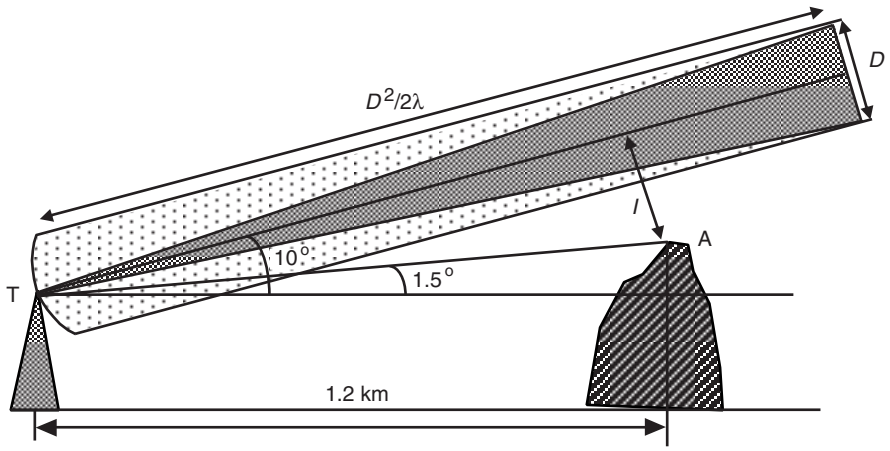

Fig. 4. Geometry showing a DSN antenna with a 10-deg elevation angle toward Madrid: the nearest hilltop has an elevation angle of 1.5 deg and a distance of 1.2 km. Note that point A is outside of the beam cylinder radiated from the antenna aperture.

antenna, a 1.2-km distance is within its near field. The side-lobe gain of the antenna in the direction of Madrid and hilltop A is actually found to be below 0 dBi [16,17].[4]

When the DSN antenna tracks a spacecraft at planetary distance, it always starts from the east and then moves toward the west at the sidereal rate of 15 deg per hour. Since Madrid and hilltop A are east of Robledo, the DSN antenna will move away from the Madrid direction at the sidereal rate, and will be about 35 deg away in 2 hours. At this angle or larger, the transmitting antenna gain would be around −7 dBi to −10 dBi according to the ITU-R model [16].

4. DSN Tracking Scenario. Figure 5 illustrates a typical scenario when the 70-m antenna at Robledo tracks a deep-space object. The Voyager 1 view period of April 11, 2002, is taken as an example (only as an example, as actual tracking did not take place). The starting point of transmission is at time $t = 0.2$ hour, when the Voyager 1 elevation angle starts to exceed 10 deg. Figure 5(a) presents the increasing angular separation between the DSN antenna beam and the direction from the antenna to Madrid. Figure 5(b) presents the effective DSN antenna gain in the direction of hilltop A. Figure 5(c) presents the estimated power transmitted by the DSN antenna and received by a mobile receiver with a 0-dBi antenna at various locations in Madrid.

At the beginning of a tracking session, the DSN antenna gain toward the Madrid direction is 0 dBi. From Eq. (4), we have $P_r = 73$ dBm − 234.4 dB = −161.4 dBm at location R, which is much below the interference thresholds of the IMT-2000 mobile receiver.

For a receiver at location M, which is on top of a tower 40 m above street level, $P_r = 73$ dBm − 177.5 dB = −104.5 dBm. At street level, the diffraction loss was calculated to be 19.8 dB larger without considering the shielding of tall buildings. The received interference power at street level, therefore, is −124.3 dBm, which also is below the receiver interference threshold.

For 75 percent of the view period, the 70-m antenna points at least 45 deg away to the west, and the antenna gain toward Madrid is around −10 dBi. At location R, $P_r = -171.4$ dBm, while $P_r = -114.5$ dBm at location M (40 m above street level) and −134 dBm at street level. These results can be seen in Figs. 5(a), 5(b), and 5(c), respectively.

[4] V. Jamnejad, "DSN Radio Frequency Interference Pattern Modeling," JPL Interoffice Memorandum (internal document), Jet Propulsion Laboratory, Pasadena, California, February 4, 1999.

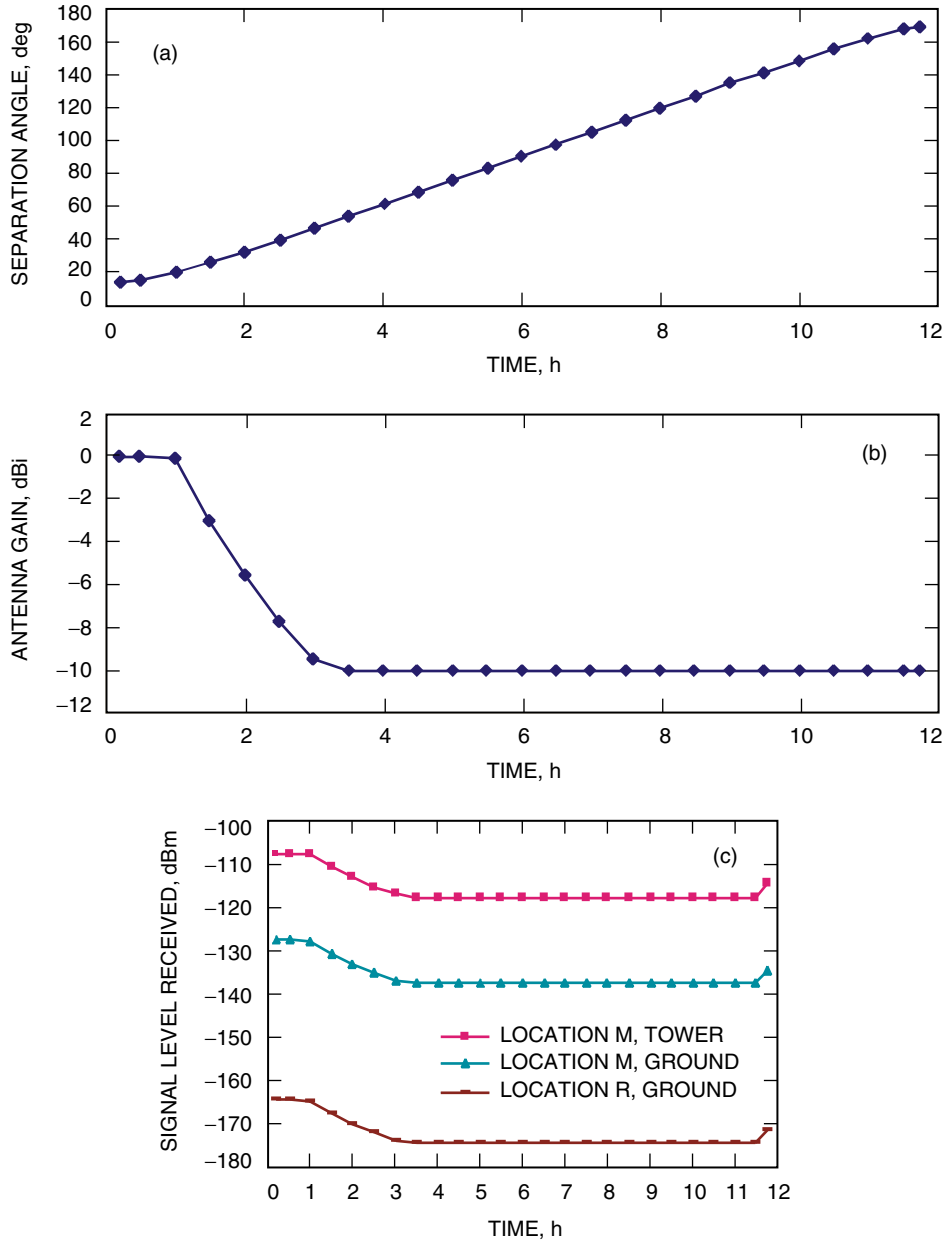

Fig. 5. Voyager 1 view period on April 11, 2002: (a) angle of separation between the DSN antenna beam and Madrid, (b) DSN antenna gain toward Madrid, and (c) estimated DSN transmitted power into a 0-dBi antenna in Madrid.

5. DSN S-Band Transmission Duty Cycle. The duty cycle of S-band (about 2-GHz) transmission from the Earth station to deep-space missions will be low. Starting in February 2002, with the Galileo mission entering the closing phase of its life, the required S-band transmission to deep-space missions will be less than 20 hours per week at Robledo. The duty cycle, therefore, will be less than 12 percent. The low duty cycle has significantly lowered the likelihood of interference.

In a rare occasion of emergency, the 70-m antenna can transmit a maximum power of $P_t = 400$ kW, raising the predicted emissions by 13 dB. Spacecraft emergency, however, has been very rare in the DSN. Past history, from 1998 to 2000, indicates that DSN stations support spacecraft emergency less than one hour per year per Complex.

6. Polarization Discrimination. The signals transmitted by the DSN are normally of circular polarization. Most mobile phone receivers, on the other hand, are linearly polarized. A receiver with linear polarization will pick up only half of the power in a circularly polarized signal, causing an effective attenuation of 3 dB. Although the polarization of the transmitted signals may not remain perfectly circular when they propagate through diffraction, atmosphere ducting, or rain scattering, the effective attenuation at the receiver is likely to be around 3 dB on average.

In estimating the power of interfering signals, we first estimated the propagation loss using standard methods, without considering polarization. The power level received by the mobile receiver then is estimated for diffraction, atmospheric ducting, and rain scattering (in Sections III, IV, and V, respectively). An additional 3 dB of attenuation is added at the end of each Section to account for polarization discrimination. In Section III, this addition is included in Figs. 5(c) and 6.

7. Estimated Interference Power versus Distance. The predicted interference power due to terrain diffraction along the Robledo–Madrid line is given in Fig. 6. The prediction is based on the normal 20-kW transmit power and transmitting antenna gains toward Madrid at the minimum (−10 dBi) and the maximum (0 dBi). The receiver is located at ground level. A polarization discrimination of 3 dB is included. It indicates that the predicted interference power in Madrid generally is below −120 dBm.

C. Comparison with Predictions of the Longley–Rice Model

The prediction based on the ITU model is compared with the Longley–Rice model [18,19] developed by the Institute of Telecommunication Sciences (ITS), which is widely used by the telecommunication industry and government agencies for interference evaluation.

Using a high-resolution (90-m, restricted data) terrain profile, and a transmitting antenna gain of −10 dBi, the Longley–Rice model generates an interference power between −175 dBm and −125 dBm around the Madrid area at street level. This is consistent with results predicted with the ITU model.

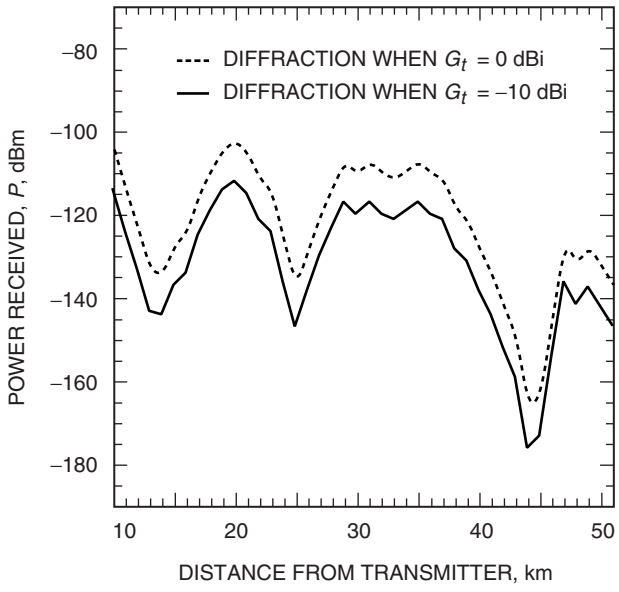

Fig. 6. The calculated received signal power at ground level through terrain diffraction along the Robledo-Madrid line, assuming a 20-kW transmitted power, a 0-dBi mobile receiver antenna gain, and a 3-dB loss due to polarization difference. The curves correspond to the maximum and minimum effective gains of the transmitting antenna in the direction of Madrid.

D. Comparison with Measurement

The office of the Secretary General of Communications conducted measurements at several locations between Robledo and Madrid of S-band emissions from the Robledo DSN station [20]. Detailed results were published in April 2000. One measurement (point M) was made in Madrid on top of the clock tower of Cibeles Palace, about 40 m from street level. The transmitter power was 225 kW, and the antenna was pointed at a 10-deg elevation angle in the azimuth direction of Madrid. The receiver antenna gain was 8 dBi. The measurement at location M was −87 dBm. Normalizing the measurement condition to 20-kW transmitter power and 0-dBi receiver antenna gain, the measured number should be −105.5 dBm (−87 dBm − 10.5 dB − 8 dB). This is very close to the predicted level at location M (the tower) under the same conditions (−107.5 dBm).

IV. Propagation by Atmospheric Ducting

Signals transmitted at an Earth station can reach beyond obstacles that block the line of sight by the mechanisms of atmospheric ducting and rain scattering, as illustrated in Fig. 7. These two mechanisms are analyzed in the following to predict the additional interference from the DSN transmitters in Robledo to the Madrid region.

As shown in Fig. 7, when the atmosphere has strong vertical gradients, slightly upward propagating waves can be trapped within the duct between the ground and a reflected atmospheric layer or within an elevated ducting layer and can propagate a long distance. As it will be shown, a hilltop higher than the transmitting antenna will significantly attenuate the signal propagated by atmospheric ducting.

Transmission loss of transhorizon ducting along the great circle of the Earth propagation is defined as [9–12,15]

$$L_1(p) = P_t + G_t + G_r - P_r \text{ (dB)} \tag{5}$$

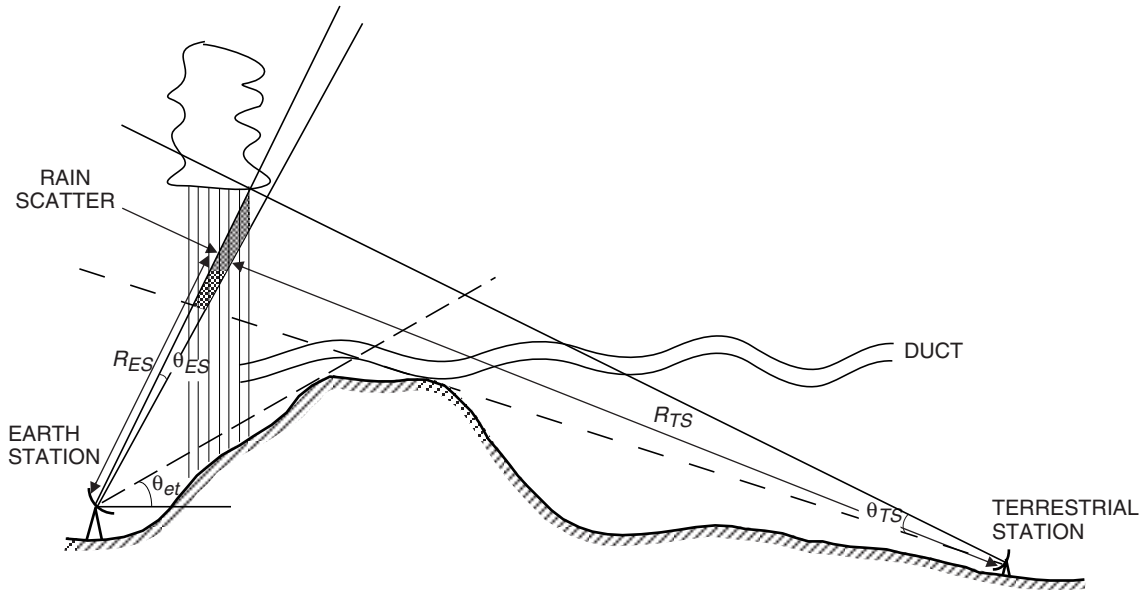

Fig. 7. Two propagation mechanisms between a DSN transmitter (Earth station) and a mobile receiver (terrestrial station) beyond the line of sight: rain scattering by a rain volume in common view and ducting propagation through a surface or elevated duct.

where p is the percentage of time of weather, assuming that the DSN antenna is transmitting. Thus, we have

$$L_1(p) = 120 + 20\log f + \gamma(p)d_1 + A_h \text{ (dB)} \tag{6}$$

where f is the signal frequency (2.11 GHz), d_1 is the distance from the transmitter (in km), and

$$\gamma(p) = 0.01 + C_1 + C_2 \log f + C_3 p^{C_4} \tag{7}$$

where C_1, C_2, C_3, and C_4 are four parameters, whose values depend on the climatic zone. The Madrid region is characterized as an A_2 radio climatic region for calculating the ducting effect, as all the land in this region is at least 50 km from the sea. A_h is an additional loss due to terrain site shielding of the transmitting station [9]:

$$A_h = 20\log\left[1 + 0.361(\theta_{et} - 0.1d_{Lt})\sqrt{f \times d_{Lt}}\right] + 0.264(\theta_{et} - 0.1d_{Lt})f^{1/3} \text{ (dB)} \tag{8}$$

where θ_{et} (in mrad) is the horizon ray elevation angle relative to the transmitter as defined in Eq. (A-2) and Fig. 7, and d_{Lt} (in km) is the distance (1.2 km) from the transmitting antenna to its radio horizon obstacle (as shown in Fig. 4). For the Robledo site, the elevation angle of the nearest hilltop, point A in Fig. 1, is 1.5 deg relative to the 70-m antenna dish center. Thus, A_h = 26.5 dB. Using the above parameters and applying Eqs. (5) through (8), and assuming that the DSN antenna is transmitting at 20 kW, the propagation loss and power received by a mobile receiver in Madrid (a distance of 50 km) is given in Table 2 as a function of percentage of time, p percent. In the last column, an additional attenuation of 3 dB is included to account for polarization discrimination.

Comparing the received powers listed in Table 2 with the interference threshold of mobile receivers, ducting effects exceed −109 dBm about 1 percent of the time, assuming that the DSN antenna is transmitting. However, since the duty cycle of S-band transmission is below 12 percent, emissions received in Madrid due to atmospheric ducting will not exceed −109 dBm more than 0.1 percent of the time. The percentage decreases with distance.

Table 2. Propagation loss and power received at Madrid through atmospheric ducting, as a function of time percentage.

p, %	Loss, L_1, dB	P_r, dBm
1.0	169.6	−109.6
2.0	172.5	−112.5
3.0	174.7	−114.7
4.0	176.4	−117.4
5.0	177.9	−117.7

V. Propagation by Rain Scattering

Rain scattering is another mode by which waves can propagate to an area beyond the line of sight. Rain droplets can reflect and scatter the waves as a mirror between a transmitter and a transhorizon receiver. Terrain has little effect on this mode, unless the mountains are so high that the rain cloud is not visible from either the transmitter or the receiver.

The rain scattering propagation loss, L_2, is defined as [10,11,21–23]

$$L_2(p) = \frac{P_t}{P_r} \tag{9}$$

The bistatic scattering equation is [22]

$$L_2 = \frac{(4\pi)^3 R_{ES}^2 R_{TS}^2}{G_{ES} G_{TS} \eta V \lambda^2} \tag{10}$$

where G_{ES} and G_{TS} refer to the gains of the Earth and terrestrial station antennas; R_{ES} and R_{TS} refer to their distances from the volume of scattering rain to the Earth and terrestrial stations, respectively; η is the radar cross section per unit volume; V is the common scattering volume; and λ is the wavelength.

Usually the Earth-station (DSN transmitting) antenna has a smaller beamwidth than the terrestrial station (UMTS receiver) antenna. The scattering volume, V, is defined by the smaller beamwidth of the two antennas:

$$V \propto \theta_{ES}^2 R_{ES}^2 \propto \frac{R_{ES}^2}{G_{ES}} \tag{11}$$

where θ_{ES} is the beamwidth of the Earth-station antenna and $\theta_{ES}^2 = \pi^2 / G_{ES}$. Thus, G_{ES} and R_{ES} are cancelled from Eq. (10), and L_2 is a function independent of G_{ES} and R_{ES}. Because of $\eta \propto \lambda^{-4}$, the transmission loss due to the rain scattering finally becomes [22]

$$L_2(p) = 168 + 20 \log R_{TS} - 20 \log f - 13.2 \log R(p) - G_{TS} + \Gamma \text{ (dB)} \tag{12}$$

where $R(p)$ is the rain rate, a function of percentage of time. Note that the Madrid region is characterized as an H rainfall climatic region on the rainfall map [9,10]. The G_{TS} of the mobile receiver is 0 dBi, and Γ is

$$\Gamma = \frac{631 k R^{\alpha}}{\sqrt{R}} 10^{-(R+1)^{0.19}} \text{ (dB)} \tag{13}$$

where k and α are two coefficients related to frequency. R_{TS} equals the distance between the transmitting antenna and the mobile receiver on average. This is because the DSN antenna does not transmit below a 10-deg elevation angle. Since the typical altitude of rain cells is about 2 km, the antenna will illuminate rain cells within 11 km of the zenith of the antenna. The distance R_{TS}, therefore, is the distance between the DSN antenna and the mobile receiver, ±11 km.

For a mobile receiver in Madrid, 50 km from the DSN antenna transmitting at 20 kW, the propagation loss and power received through rain scattering are calculated by Eqs. (12) and (9) and are given in

Table 3 as a function of percentage of time, p percent. The last column has included an additional 3 dB of attenuation due to the polarization difference.

Comparing the power calculated above with the receiver threshold, we can see that the expected effect of rain scattering on a mobile receiver in Madrid does not exceed the threshold of −109 dBm more than 0.1 percent of the time, assuming that the DSN antenna is transmitting. Given that the duty cycle of the S-band transmission is below 12 percent, the threshold will not be exceeded more than 0.01 percent of the time.

Note that the received power estimated here is much lower than the estimates in a previous analysis [12] as a result of using the correct antenna gain of a mobile receiver.

Table 3. Propagation loss and power received at Madrid through rain scattering, as a function of time percentage.

p, %	Loss, L_2, dB	P_r, dBm
0.1	181.6	−111.6
1.0	190.7	−120.7
2.0	197.2	−127.2

VI. Atmospheric Ducting and Rain Scattering at Larger Distances

Figure 8 summarizes interference powers generated through ducting and rain scattering modes as a function of distance for various time percentages, p, assuming the antenna is transmitting. An additional attenuation of 3 dB is included for the polarization difference.

Note that the estimation of the ducting effect given in Fig. 8 applies not only to locations between Robledo and Madrid, which are shielded by hilltop A, but also to locations in other directions, which are shielded by hilltops similar to hilltop A. The estimation for rain scattering in Fig. 8 applies to all areas around Robledo because hills in this region are not high enough to affect rain scattering.

Another way to look at Figure 8 is the following. When the Robledo 70-m antenna is transmitting at 20 kW, emissions propagated via atmospheric ducting or rain scattering are not expected to exceed the power levels given in Table 4 more than 1 percent of the time. Considering the 12 percent duty cycle of Robledo S-band transmission, these power levels will not be exceeded more than 0.1 percent of the time on a weekly or yearly basis. Note that all these power levels are below the mobile receiver interference thresholds of −109 dBm.

VII. Conclusion

This analysis shows that hills to the east of the DSN antennas at Robledo provide significant attenuation to the S-band emissions that are transmitted by the DSN antennas and propagated toward Madrid by diffraction over the terrain or ducting through atmospheric layers. The emissions from a 20-kW DSN transmitter propagated by diffraction will reach the ground level of Madrid at a received power lower than the −109-dBm interference threshold of the UMTS mobile receiver. This is shown in Fig. 5 over the entire view period of a typical deep-space tracking session. Estimation of received emission levels via diffraction is given in Fig. 6 as a function of distance along the Robledo–Madrid line.

The emissions propagated via atmosphere ducting or rain scattering are not expected to exceed the power levels given in Table 4 more than 0.1 percent of the time, taking into account the low duty cycle

(12 percent) of DSN S-band transmission. The effects decrease with distance, as shown in Fig. 8. Relative to the interference threshold of a UMTS mobile receiver, the expected effect of atmospheric ducting will not exceed the threshold more than 0.1 percent of the time in the city of Madrid. The expected effect of rain scattering will not exceed the threshold more than 0.01 percent of the time in that city.

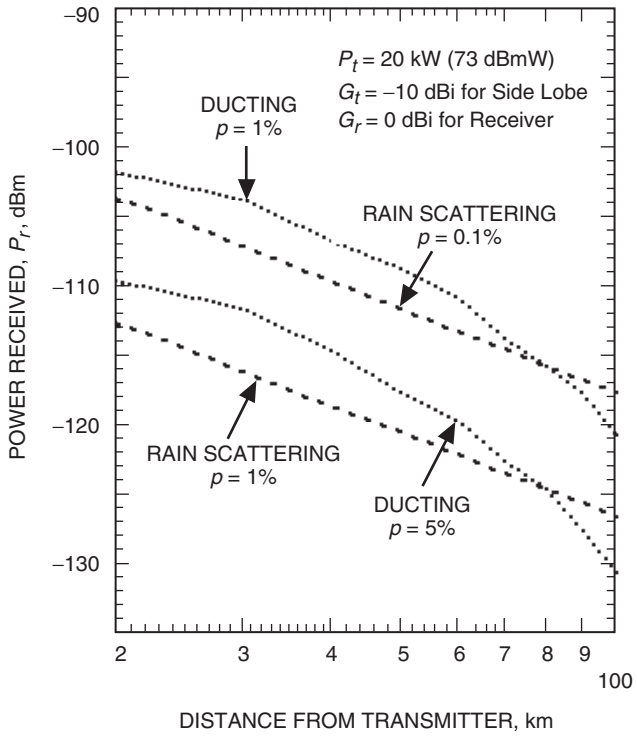

Fig. 8. Received powers through atmospheric ducting and rain scattering as a function of distance from the DSN transmitter at Robledo for various percentages of time, assuming the DSN antenna is transmitting.

Table 4. Emission levels exceeded for 1 percent of the time during continuous transmission (equivalent to 0.1 percent of the time on a weekly basis considering the low duty cycle of transmission).

Propagation mode	Power level, dBm	
	Distance from Robledo	
	50 km	100 km
Atmospheric ducting	−110	−121
Rain scattering	−121	−127

Acknowledgments

We would like to thank G. Hand and P. McKenna of the Institute of Telecommunication Sciences for providing a prediction using the Longley–Rice model, D. Bathker of JPL for consultation on near-field antenna radiation patterns, F. Morgan, also of JPL, for graphic assistance, and A. Kantak (JPL) for reviewing this article.

References

[1] International Telecommunication Union, "International Mobile Telecommunications-2000 (IMT-2000)," Recommendation ITU-R M.687, 1997.

[2] International Telecommunication Union, "Framework for Services Supported on International Mobile Telecommunications-2000 (IMT-2000)," Recommendation ITU-R M.816, 1997.

[3] International Telecommunication Union, "Guidelines for Evaluation of Radio Transmission Technologies for IMT-2000," Recommendation ITU-R M.1225, 1997.

[4] "ITU Finds Way Forward for 3G Mobile Systems," *ITU News,* p. 18, 4/99, 1999.

[5] International Telecommunication Union, "Spectrum Considerations for Implementation of International Mobile Telecommunications-2000 (IMT-2000) in the Band 1885–2025 MHz and 2110–2200 MHz," Recommendation ITU-R M.1036, 1999.

[6] "European Radiocommunications Committee Decision on the Harmonized Utilization of Spectrum for Terrestrial Universal Mobile Telecommunications System (UMTS) Operating within the Bands 1900–1980 MHz, 2010–2025 MHz and 2110–2170 MHz," ERC 25th meeting, Helsinki, Finland, March 10–12, 1999.

[7] T. Ojanpera and R. Prasad, "An Overview of Third-Generation Wireless Personal Communications: A European Perspective," *IEEE Personal Communications,* vol. 36, p. 59, December 1998.

[8] E. Dahlman, B. Grudmundson, M. Nilsson, and J. Skold, "UMTS/IMT-2000 Based on Wideband CDMA," *IEEE Communications Magazine,* vol. 36, p. 70, September 1998.

[9] International Telecommunication Union, "Prediction Procedure for the Evaluation of Microwave Interference between Stations on the Surface of the Earth at Frequencies above about 0.7 GHz," Recommendation ITU-R P.452-9, 1999.

[10] International Telecommunication Union, "Determination of the Coordination Area of an Earth Station Operating with a Geostationary Space Station and Using the Same Frequency Band as a System in a Terrestrial Service," Recommendation ITU-R IS.847-1, 1993.

[11] International Telecommunication Union, "Propagation Data Required for the Evaluation of Coordination Distances in the Frequency Range 100 MHz to 105 GHz," Recommendation ITU-R P.620-4, 1999.

[12] C. Ho, M. Sue, T. Peng, P. Kinman, and H. Tan, "Interference Effects of Deep Space Network Transmitters on IMT-2000/UMTS Receivers at S-Band," *The Telecommunications and Mission Operations Progress Report 42-142, April–June 2000,* Jet Propulsion Laboratory, Pasadena, California, pp. 1–21, August 15, 2000.
http://tmo.jpl.nasa.gov/tmo/progress_report/42-142/142A.pdf

[13] International Telecommunication Union, "Propagation by Diffraction," Recommendation ITU-R P.526-6, 1999.

[14] International Telecommunication Union, "Attenuation by Atmospheric Gases," Recommendation ITU-R P.676-4, 1999.

[15] International Telecommunication Union, "Method for the Determination of the Coordination Area Around an Earth Station in Frequency Bands between 1 GHz and 40 GHz Shared between Space and Terrestrial Radiocommunication Services," Appendix S7 (former Appendix 28), *Radio Regulations,* Geneva, Switzerland: ITU, 1990 edition, revised 1997.

[16] International Telecommunication Union, "Mathematical Model of Average and Related Radiation Patterns for Line-of-Sight Point-to-Point Radio-Relay System Antennas for Use in Certain Coordination Studies and Interference Assessment in the Frequency Range from 1 GHz and to about 70 GHz," Recommendation ITU-R F.1245-1, 2000.

[17] J. F. Ramsay, "Tubular Beams from Radiating Apertures," *Advances in Microwaves,* vol. 3, edited by L. Young, New York: Academic Press, 1968.

[18] P. L. Rice, A. G. Longley, K. A. Norton, and A. P. Barsis, *Transmission Loss Predictions for Tropospheric Communication Circuits,* vol. I, Technical Note 101, National Bureau of Standards, U.S. Department of Commerce, Washington, D.C., January 1, 1967.

[19] P. L. Rice, A. G. Longley, K. A. Norton, and A. P. Barsis, *Transmission Loss Predictions for Tropospheric Communication Circuits,* vol. II, Technical Note 101, National Bureau of Standards, U.S. Department of Commerce, Washington, D.C., January 1, 1967.

[20] Ministerio De Fomento, Secretaria General De Communicaciones, *Medidas De Cobertura Radioelectrica, Antenna DSS-63, MDSCC,* Noviembre 1999.

[21] R. K. Crane, "A Review of Transhorizon Propagation Phenomena," *Radio Science,* vol. 16, p. 649, 1981.

[22] W. L. Flock, *Propagation Effects on Satellite Systems at Frequencies below 10 GHz, A Handbook for Satellite Systems Design,* NASA Reference Publication 1102, 1987.

[23] International Telecommunication Union, International Radio Consultative Committee (CCIR), "Scattering by precipitation," Report 882-1, *Propagation in Nonionized Media, Recommendations and Reports of the CCIR,* vol. V, Geneva, Switzerland, 1986.

[24] *CEPT European Radiocommunications Committee Report 65*, Helsinki, Finland, November 1999.

Appendix
Calculation of Diffraction Losses

I. Diffraction over Two Isolated Obstacles

Referring to Fig. 3 in the main text, there is only one obstacle blocking the line of sight from the transmitter at location T to the receiver at location M, but there are two isolated obstacles blocking the direct line of sight from location T to location R. Based on the method of estimating diffraction losses involving two isolated obstacles recommended in ITU-R P.526 [13], the total diffraction loss is the sum of two terms. The first term is the diffraction loss due to ridge A, along a path from T to A to B, over distances a and b (transmitter T − first ridge A − second ridge B). The second term is the loss due to obstacle B, along a path from A to B to R, over distances b and c (first ridge A − second ridge B − location R). The two terms then are added together to obtain the total diffraction attenuation over the entire path. A small correction term L_c is also added to take into account the separation b between the edges. This method is illustrated in Fig. A-1.

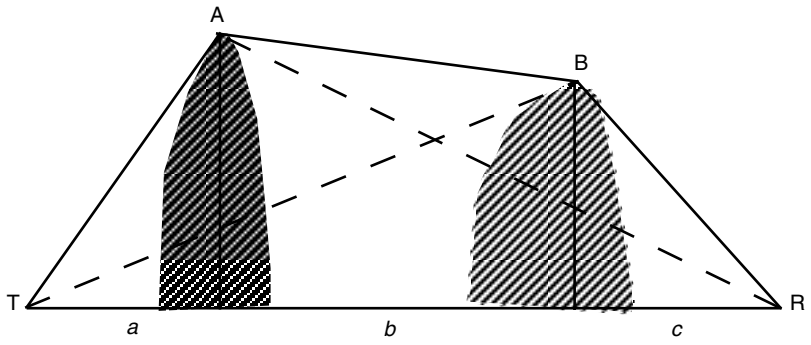

Fig. A-1. Geometry for calculating diffraction losses over double isolated edges.

II. Loss over Obstacle A

First, we calculate the diffraction loss over peak A in Fig. 3. The peak is approximated by a rounded knife edge with a thickness of 300 m (the separation of the small twin peaks). As we will show later, thickness contributes significantly to loss. The angular distance, θ, is the angle in radians between horizon rays TA and BA (or MA) in the great circle plane:

$$\theta = \frac{d}{a_e} + \theta_{et} + \theta_{er} \tag{A-1}$$

where d is the distance between the transmitter and receiver at sea level and a_e is the median effective Earth radius. The horizon ray elevation angles θ_{et} relative to the transmitter and θ_{er} relative to the receiver may be computed using the following equations:

$$\theta_{et} = \frac{h_{Lt} - h_{ts}}{d_{Lt}} - \frac{d_{Lt}}{2a_e} \tag{A-2}$$

and

$$\theta_{er} = \frac{h_{Lr} - h_{rs}}{d_{Lr}} - \frac{d_{Lr}}{2a_e} \tag{A-3}$$

where h_{Lt} and h_{Lr} are the elevations of horizon obstacles and h_{ts} and h_{rs} are the elevations of the transmitting and receiving antennas, respectively, all above the average mean sea level (AMSL). The transmitter antenna is 37 m above the ground, while the receiver at location R in Madrid is 1.5 m above the ground, and the receiver at the top of the clock tower of Cibeles Palace (location M) is about 40 m above the ground. The d_{Lt} and d_{Lr} are sea level arc distances from each antenna to their radio horizon obstacles, respectively. The location of the radio obstacle relative to the transmitter (h_{Lt}, d_{Lt}) or the receiver (h_{Lr}, d_{Lr}) is determined by seeking the maximum elevation angle calculated by Eq. (A-2) or Eq. (A-3). The horizon elevation angle is defined here as the angle viewed from the center of the Earth-station antenna, between the horizontal plane and a ray that grazes the visible physical horizon in the direction concerned; d_1 and d_2 are the distances from the transmitter and receiver, respectively, to the top of the peak. For practice, d_1 and d_2 may be replaced by d_{Lt} and d_{Lr}, because the peak height is relatively small compared to the horizontal distance. D_s (300 m) is the thickness of the obstacle, and h_r is its height relative to the baseline TB or TM. All parameters for this study are listed in Table A-1 for peak A and are also shown in Fig. A-2.

For a rounded obstacle, the diffraction loss includes two parts:

$$A = J(\nu) + T(m, n) \tag{A-4}$$

where $J(\nu)$ is a loss due to an equivalent knife edge placed with its peak at the vertex point, while $T(m, n)$ is the additional loss due to the curvature of the obstacle. Parameters m and n are defined later.

Table A-1. Path parameters for the geometry involving obstacle A.

Path	d, km	d_1, km	d_2, km	d_{Lt}, km	d_{Lr}, km	h_{ts}, km	h_{rs}, km	h_{Lt}, km	h_{Lr}, km	h_r, km	D_s, km
TAB	38.8	1.2	37.6	1.2	37.6	0.865	0.700	0.896	0.896	0.031	0.30
TAM	47.3	1.2	46.1	1.2	46.1	0.865	0.680	0.896	0.896	0.031	0.30

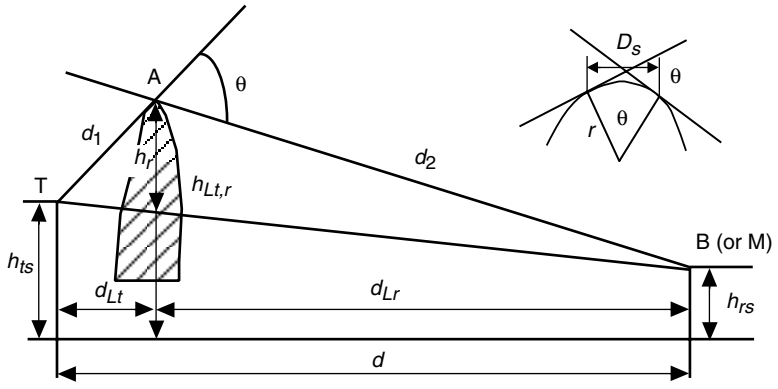

Fig. A-2. Geometric parameters for calculating diffraction losses relative to point B (or M) caused by a rounded obstacle. The inserted diagram in the upper right shows the thickness, D_s, and the radius of the rounded obstacle.

To calculate $J(\nu)$, we need to first evaluate parameter ν, which is defined as

$$\nu = \theta \sqrt{\frac{2d_1 d_2}{\lambda d}} \tag{A-5}$$

where angular distance, θ, is from Eq. (A-1) and wavelength $\lambda = 1.42 \times 10^{-4}$ km for the radio wave at S-band (2115 MHz). The diffraction loss for a single knife edge is

$$J(\nu) = 6.9 + 20 \log \left(\sqrt{(\nu - 0.1)^2 + 1} + \nu - 0.1 \right) \text{ (dB)} \tag{A-6}$$

Then we calculate radius r of the rounded knife edge:

$$r = \frac{D_s}{\theta} \tag{A-7}$$

where D_s is the thickness of the rounded knife edge.

The curvature loss is

$$T(m, n) = k(n) \times m^{b(n)} \tag{A-8}$$

where

$$m = \frac{r \left[\frac{d_1 + d_2}{d_1 d_2} \right]}{\left(\frac{\pi r}{\lambda} \right)^{1/3}} \tag{A-9}$$

$$n = \frac{h_r \left[\frac{\pi r}{\lambda} \right]^{2/3}}{r} \tag{A-10}$$

$$b = 0.73 + 0.27 \left[1 - \exp \left(-1.43n \right) \right] \tag{A-11}$$

and

$$k = 8.2 + 12.0n \tag{A-12}$$

Using the median effective Earth radius, Eqs. (A-1) through (A-12), and the parameters listed in Table A-1, we obtain values for $\theta, \nu, J(\nu)$, curvature loss T, and diffraction loss A with respect to point B and location M, as presented in Table A-2. Note that the two sets of numbers are very close.

Table A-2. Calculated loss parameters for paths TAB and TAM due to obstacle A.

Path	θ, rad	ν	$J(\nu)$, dB	r, km	m	n	b	k	T, dB	A, dB
TAB	0.0333	4.257	25.42	9.0	0.129	11.75	1.0	149.4	19.20	44.62
TAM	0.0331	4.250	25.40	9.0	0.132	11.75	1.0	149.2	19.66	45.06

III. Loss over Obstacle B

There is no diffraction loss between peak A and a receiver at location M because peak B, an isolated rounded obstacle, does not block the line of sight. However, there is diffraction loss from peak A to location R due to obstacle B. The mountain ridge B may be approximated as a rounded obstacle. The geometry for an idealized rounded obstacle is shown in Fig. A-3. Here, the rounded obstacle is isolated from the surrounding terrain. We have used a two-dimensional cylinder with radius r to represent the rounded obstacle B.

Two straight lines from points A and R tangential to the cylinder cross each other at point B, as shown; h_r is the obstacle's height from point B to the baseline AR; D_s is the horizontal distance between two tangent points on the cylinder; d_{st} is the horizontal distance from point B to the tangential point on the left; and d_{sr} is the horizontal distance to the tangential point on the right. All parameters for the calculation of diffraction loss over obstacle B are given in Table A-3.

For a large rounded obstacle, the radius is obtained using

$$r = \frac{2D_s d_{st} d_{sr}}{\theta_2 (d_{st}^2 + d_{sr}^2)} \tag{A-13}$$

where

$$D_s = d_{st} + d_{sr} \tag{A-14}$$

Using the median effective Earth radius, obtained from Eqs. (A-13) and (A-14), equations given in the previous subsections, and parameters in Table A-3, we obtain the results given in Table A-4.

IV. Combined Diffraction Losses from the Transmitter to the Receiver

The total diffraction loss from transmitter T to the receiver at location R is the combination of losses due to both obstacles A and B, as shown in Fig. A-1 [13]:

$$L_d = A_{\mathrm{TAB}} + A_{\mathrm{ABR}} + L_c \tag{A-15}$$

where L_c is a correction term (=0.02 dB). From values of A in Tables A-2 and A-4, we have $L_d = 102.46$ dB for a receiver at location R. For a receiver at location M, there is only one obstacle, A_{TAM}, and the loss $L_d = 45.06$ dB, from Table A-2.

The actual diffraction loss conceivably is greater than the theoretical loss calculated here because of other possible terrain effects, such as surface roughness, clutter, etc., which are not included in this model. These factors usually can cause an additional loss of around 10 dB [18,19].

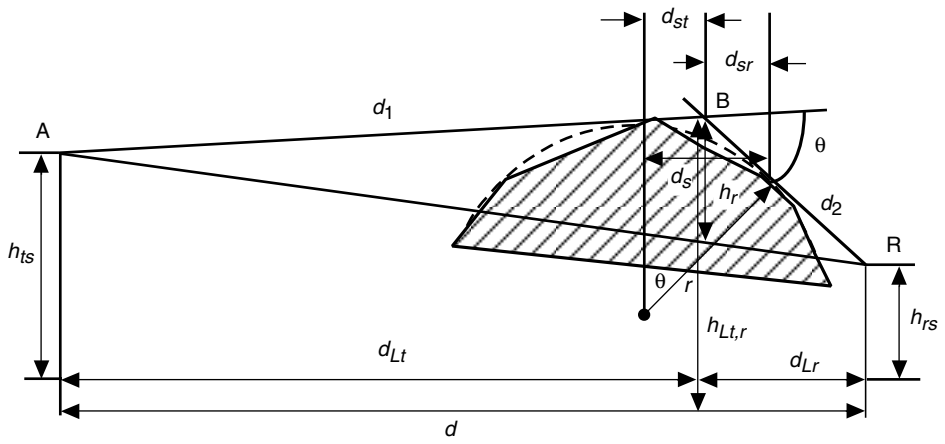

Fig. A-3. Geometric parameters for calculating diffraction loss from peak A to location R due to a large rounded obstacle B.

Table A-3. Path parameters for the geometry involving peak B.

d, km	d_1, km	d_2, km	d_{Lt}, km	d_{Lr}, km	h_{ts}, km	h_{rs}, km	h_{Lt}, km	h_{Lr}, km	d_{st}, km	d_{sr}, km	h_r, km
43.5	37.6	5.9	37.6	5.9	0.896	0.587	0.700	0.700	2.2	3.0	0.07

Table A-4. Calculated loss parameters for path ABR due to obstacle B.

Path	θ, rad	ν	$J(\nu)$, dB	r, km	m	n	b	k	T, dB	A, dB
ABR	0.0164	4.40	25.70	301.8	0.310	8.24	1.0	107.1	32.12	57.82

Total propagation losses through the terrain diffraction are

$$L = L_b + L_d \tag{A-16}$$

where L_b is free-space transmission loss due to distance d,

$$L_b = 32.45 + 20 \log f + 20 \log d \tag{A-17}$$

where frequency f is in MHz and distance d is in km. Thus, for a receiver at location R, we have $L_b = 131.96$ dB and, with the diffraction loss L_d calculated above, $L = 234.40$ dB. Here we have neglected the gaseous absorption loss in the surface [14] because this loss is very small at S-band.

For a receiver at location M, $L_b = 132.46$ dB. We then have $L = 177.52$ dB. Note the large difference between propagation losses from the same transmitter to two receivers at locations R and M, which are only 2.6 km apart, because of the existence of a second obstacle along the path.

V. Statistical Distribution due to Atmospheric Gradients

Diffraction loss is a function of the effective Earth radius, a_e, which depends on the changing atmospheric refractivity gradients. Diffraction loss, therefore, has a statistical distribution as a result of uncertainty in the atmosphere refractivity.

At 50 percentile, $p = 50$ percent, and $L_d(50\%)$ is computed using the median effective Earth radius, $a_e(50\%)$. The median diffraction loss is $L_d(50\%) = 102.46$ dB for the receiver at location R.

For a very small percentage of time when the refractivity index gradient becomes very large, an anomalous effective Earth radius applies. The anomalous time percentage, $\beta_0(\%)$, is defined as the percentage of time when the refractivity index gradient exceeds 100 N-units/km in the first 100 m of the lower atmosphere at the central latitude, φ, under consideration:

$$\beta_0 = 10^{-0.015|\varphi|+1.67}\mu_1\mu_2 \ (\%) \tag{A-18}$$

where μ_1 and μ_2 are parameters depending on the degree to which the path is over land and water. For the Madrid–Robledo path, where $\varphi = 40$ deg, we have $\mu_1 = 0.144$, $\mu_2 = 1.566$, and $\beta_0 = 2.64$ percent. In this case, k_{β_0} is 2.8, per Eq. (1) [9], and the anomalous effective Earth radius is $a_e(\beta_0) = 6371 \times k_{\beta_0} = 19,113$ km, per Eq. (2).

For $p \leq \beta_0$ percent, $L_d(\beta_0)$ is computed using the anomalous effective Earth radius, $a_e(\beta_0)$, for an anomalous time percentage, $\beta_0(\%)$. Following the same procedure as used in the previous sections, we have anomalous diffraction loss $L_d(\beta_0) = 99.5$ dB, which is only 2.9 dB less than the median diffraction loss.

For $\beta_0\% < p < 50\%$, $L_d(p)$ is given by [9]

$$L_d(p) = L_d(50\%) - F_i(p)\,[L_d(50\%) - L_d(\beta_0)] \tag{A-19}$$

where $F_i(p)$ is an interpolation factor based on a log-normal distribution of diffraction loss over the range $\beta_0\% < p < 50\%$, given by

$$F_i(p) = \frac{I\left(\frac{p}{100}\right)}{I\left(\frac{\beta_0}{100}\right)} \tag{A-20}$$

where $I(p/100)$ is the inverse cumulative normal function.

Finally, the total propagation loss as a function of percentage of time, p, is

$$L(p) = L_b + L_d(p) \tag{A-21}$$

where we have neglected a small correction term, $E_{sd}(p)$. The result for a receiver at location R is shown in Fig. A-4. We can conclude that the propagation loss due to diffraction is almost constant throughout the year.

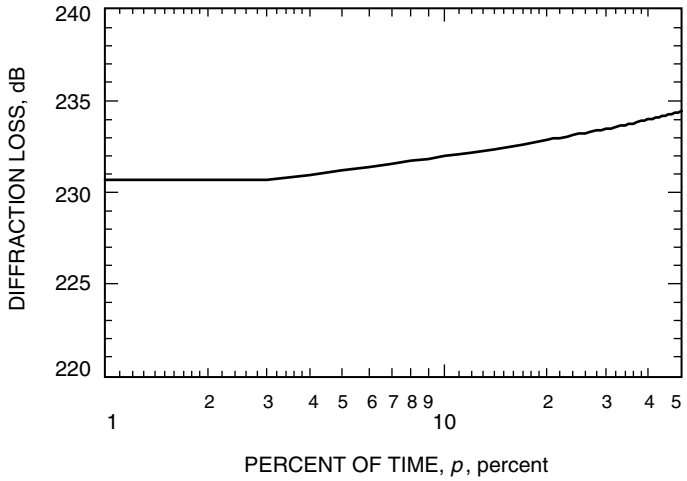

Fig. A-4. Total diffraction loss over two obstacles from a transmitter at location T to a receiver at location R as a function of time percentage.